131 Hartwell Avenue
Lexington, Massachusetts
02421-3126
USA
Tel: +1 781 761-2288
Fax: +1 781 761-2299
www.aer.com

FINAL REPORT

AQRP Project 22 - 003
Evaluating the Ability of Statistical and Photochemical Models to Capture the Impacts of Biomass Burning Smoke on Urban Air Quality in Texas

Revision 2.0

Prepared by:
Jennifer Hegarty, Chase Calkins, John Henderson, Richard Pernak,
and Matthew Alvarado
Atmospheric and Environmental Research, Inc. (AER)
131 Hartwell Ave.
Lexington, MA 02421-3126

Correspondence to: malvarad@aer.com

Prepared for:
Texas Air Quality Research Program (AQRP)
The University of Texas at Austin

August 31, 2023

Document Change Record

Revision	Revision Date	Remarks
1.0	6 August 2023	Draft Submitted to the TCEQ
2.0	31 August 2023	Revised Version Submitted to the TCEQ

Acknowledgements

This research report was supported by funding from the Texas Commission on Environmental Quality (TCEQ). The findings, opinions, or conclusions expressed do not necessarily represent those of the TCEQ.

Disclaimer: The information contained in this report or deliverable has not been evaluated by EPA for this specific application.

TABLE OF CONTENTS

List of Figures

List of Tables

List of Acronyms

CAMx – Community Atmosphere Model with Extensions
ELP – El Paso
EPA – Environmental Protection Agency
GAM – Generalized Additive Model
HGB – Houston-Galveston-Brazoria
MDA8 – Maximum Daily 8-hour Average
QAPP – Quality Assurance Project Plan
STILT – Stochastic Time-Inverted Lagrangian Transport
TCEQ – Texas Commission on Environmental Quality
WRF – Weather Research and Forecasting Model

Executive Summary

The objectives of this project were to:

(1) Use generalized additive models (GAMs) driven with satellite and surface observations to examine the impact of fires on background and total O_3 and $PM_{2.5}$ in Texas urban areas.

(2) Examine the ability of CAMx photochemical model to simulate these fire impacts by applying similar statistical methods to the CAMx results.

(3) Use any statistically significant differences found to prioritize different approaches to improve the ability of CAMx to simulate the impacts of domestic fires on air quality.

We performed a statistical analysis using generalized additive models (GAMs) to see how fires impacted background and maximum concentrations of O_3 and $PM_{2.5}$ in Houston and El Paso. Our results suggest that on days when the HMS indicated smoke over Houston and El Paso, the daily average $PM_{2.5}$ was elevated by 1.4-2.6 μg/m^3 on average (background and maximum) while the background MDA8 O_3 was elevated by 2.4-8 ppbv on average. Unfortunately, the results depend strongly on which set of fire predictors is used. For Houston, the change in O_3 impact as the smoke enters the city varies from -0.9 ppbv to +6.0 ppbv, with three out of four methods predicting an increase in mean O_3 as the smoke enters the city. In El Paso, the change in mean O_3 impact as the smoke enters the city varies from -1.6 ppbv to -0.5 ppbv. The geographic fire variables from Sec. 4.1.3 give the best fitting statistics and predicts fire impacts of 7.0-8.0 ppbv in both urban areas, with a slight decrease in the impact when the smoke enters the city.

We also performed a statistical analysis using generalized additive models (GAMs) to see if the CAMx predictions were consistent with the impact of fires on background and maximum concentrations of O_3 in Houston and El Paso. For El Paso, our analysis suggested that there were statistically significant differences between CAMx and the ambient data, but further analysis showed that the predicted impacts of fires in both cases were very similar. For Houston, however, the differences between CAMx and the ambient data fits were not statistically significant for maximum O_3, but the CAMx data strongly overestimates the background O_3 for Houston on both smoky and non-smoky days.

Since CAMx generally appears to give similar predictions for the impacts of smoke as the ambient data, there is little need to identify areas for improvement as called for in Objective 3 of this project. The exception is for the impacts of smoke on Houston background O_3, where CAMx predicts a 2 ppb larger impact. This is likely related to the general large overestimate of background O3 by CAMx in Houston but may also be due to errors in the chemistry as emissions from the Yucatan interact with halogens over the Gulf.

In addition, our results showed that CAMx overestimates Houston background O_3 on both smoky and non-smoky days, suggesting that further work needs to be done on ozone-destroying halogen emissions and chemistry and on the biogenic emissions upwind of Houston. Similarly, the underpredictions of maximum O_3 in El Paso suggest that further work is needed on CAMx emissions for El Paso and Ciudad Juarez and the O_3 chemistry within the combined urban area.

Future work should focus on finding ways to better determine the best set of smoke predictors for use in statistical studies such as this, with a focus on high tail events where smoke could lead to an exceedance of air quality standards using methods from Brown-Steiner et al. (2021). While the predictions of smoke impact on O_3 from CAMx appear to be reasonable based on this study, our results suggest that further work is needed to (a) address the overestimate of Houston background O_3 on both smoky and non-smoky days and (b) the underpredictions of maximum O_3 in El Paso.

1 Introduction

Understanding the impact of domestic fire smoke on urban air quality (AQ) requires understanding (i) the chemistry of the smoke before it reaches the city and (ii) the changes in the urban production rate of O_3 and $PM_{2.5}$ caused by the smoke. The relative importance of these two pathways on the air quality impacts of domestic fire smoke is not well understood and it is unclear which processes should be targeted to reduce the overall uncertainty.

In addition, three-dimensional (3D) photochemical models like CAMx can have trouble representing the near-source chemistry of the smoke plume and the impact of smoke mixing with urban pollution due to a combination of low spatial resolution near fires and incorrect representation of the chemistry of smoke-specific VOCs (e.g., Baker et al., 2016). These limitations in physical approaches have led to the development of a variety of statistical approaches to estimate the impact of biomass burning on urban AQ (e.g., Gong et al., 2017; de Foy et al., 2021). However, little work has been done to compare the statistical and 3D photochemical approaches or to identify priorities for further development of both approaches. Thus, the US EPA and US Forest Service organized assessment of smoke research needs noted this was a key priority for future smoke chemistry research (Alvarado et al., 2022).

Thus, the objectives of this project are to:

(1) Use generalized additive models (GAMs) driven with satellite and surface observations to examine the impact of fires on background and total O_3 and $PM_{2.5}$ in Texas urban areas.

(2) Examine the ability of CAMx photochemical model to simulate these fire impacts by applying similar statistical methods to the CAMx results.

(3) Use any statistically significant differences found to prioritize different approaches to improve the ability of CAMx to simulate the impacts of domestic fires on air quality.

In this final report, we examine the impact of fires on urban AQ in Texas using statistical modeling (Objective 1) and the ability of CAMx photochemical model to simulate these fire impacts by applying similar statistical methods to the CAMx results (Objective 2). Two urban areas were examined: Houston-Galveston-Brazoria (HGB) and El Paso. Background O_3 and $PM_{2.5}$ concentrations were estimated using the lowest value observed at sites near the border of the area of interest, as TCEQ has done in the past (e.g., Berlin et al., 2013). Analyzing the impacts of fires on background and urban sites separately allows us to examine the change in O_3 and $PM_{2.5}$ due to the mixing of smoke with urban pollution separately from the impact of smoke before it mixes with urban pollution.

Below we discuss the dataset for this project, including the smoke and fire predictors developed so far for this project (Section 2), the statistical modeling approach (Section 3), and our initial findings (Section 4). Section 5 discusses our QA findings, Section 6 summarizes our conclusions, and Section 7 describes our plans for future research.

2 Dataset for Model Training

2.1 Ambient Air Quality Data

Maximum daily 8-hour average (MDA8) O_3 mixing ratios and daily average $PM_{2.5}$ concentrations will be calculated for each HGB and El Paso site from the surface air quality data in TAMIS. Sites in each urban area were separated into background (for sites on the outskirts of the city) and urban (for sites near the city core). For each urban area, the minimum value of MDA8 O_3 and daily average $PM_{2.5}$ from background sites upwind of the urban core were selected as the background estimate for that day, while the maximum concentrations were selected as the urban maximum.

2.2 Meteorological Predictors

The meteorological predictors to be used in this study (Table 1) are based on our previous GAM studies of the ability of meteorological predictors to estimate the concentrations of O_3 and $PM_{2.5}$ at urban and background monitoring sites in Texas. Our team has shown that these meteorological predictors, plus the previous day's MDA8 O_3 or daily average $PM_{2.5}$, can explain approximately 70% of the variability in background and urban O_3, and about 30-40% of the variability in background and urban $PM_{2.5}$ (e.g., Alvarado et al., 2015; McVey et al., 2018; Pernak et al., 2019; Brown-Steiner et al., 2021).

Table 1. Meteorological parameters used in the GAMs. The column name is given in italics.

1) Afternoon mean temperature (°C, *afternoon_mean_T, 1-4 PM CST*)
2) Diurnal temperature change (°C, *diurnal_T*)
3) Daily average wind speed (m/s, *daily_ws*)
4) Daily average wind direction (degrees clockwise from North, *daily_wd*)
5) Daily average water vapor density (g/m^3, *SWVP*)
6) Morning surface temperature difference (1200 UTC) (temperature at 925 or 700 mb–temperature at surface at 1200 UTC) (°C, *T_dif_925mb* or *T_dif_700mb*)
7) Transport direction (degrees clockwise from North, *HYSPLIT_Bearing*)
8) Transport distance (m, *HYSPLIT_dist*)

Variables 1-5 in Table 1 were calculated from the surface meteorological data in the Texas Air Monitoring Information System (TAMIS). Variable 6, which reflects the vertical stability of the atmosphere each day, was calculated from upper atmosphere data in the Integrated Global Radiosonde Archive (IGRA Version 2). Given El Paso's higher elevation, an upper atmosphere level of 700 mbar was used for this city as opposed to the 925 mbar value used for all other urban areas. Variables 7 and 8 were calculated from 24-hour NOAA Hybrid Single-Particle Lagrangian Integrated Trajectory model (HYSPLIT) back-trajectories driven with 12 km horizontal resolution NAM data. As in Camalier et al. (2007), these back-trajectories are calculated assuming an initial height of 300 m above ground level (AGL) and are started at noon local solar time. The endpoints of the back-trajectories were used to calculate the 24-hour transport direction and distance for each urban area for the 2012-2021 period.

2.3 Fire and Smoke Predictors

The NOAA Hazard Mapping System (HMS) Fire and Smoke product will be our primary source of fire predictors, as we have shown that days where the HMS product indicates smoke over Houston tend to be associated with enhancements in CO, O_3, NO_x, and NO_y (Figure 1). This gives us confidence in the ability of our statistical modeling to be able to identify a statistically significant impact of fires on air quality in HGB and El Paso. To make the HMS, satellite analysts compare automated fire detections to the infrared satellite images used to produce them to ensure each fire exists (Ruminski et al., 2006; Schroeder et al., 2008; Brey et al., 2018). Small fires are more difficult to detect and are underreported (*e.g.*, Hu et al., 2016). False fire detections are removed, and fires that were not automatically detected are added manually.

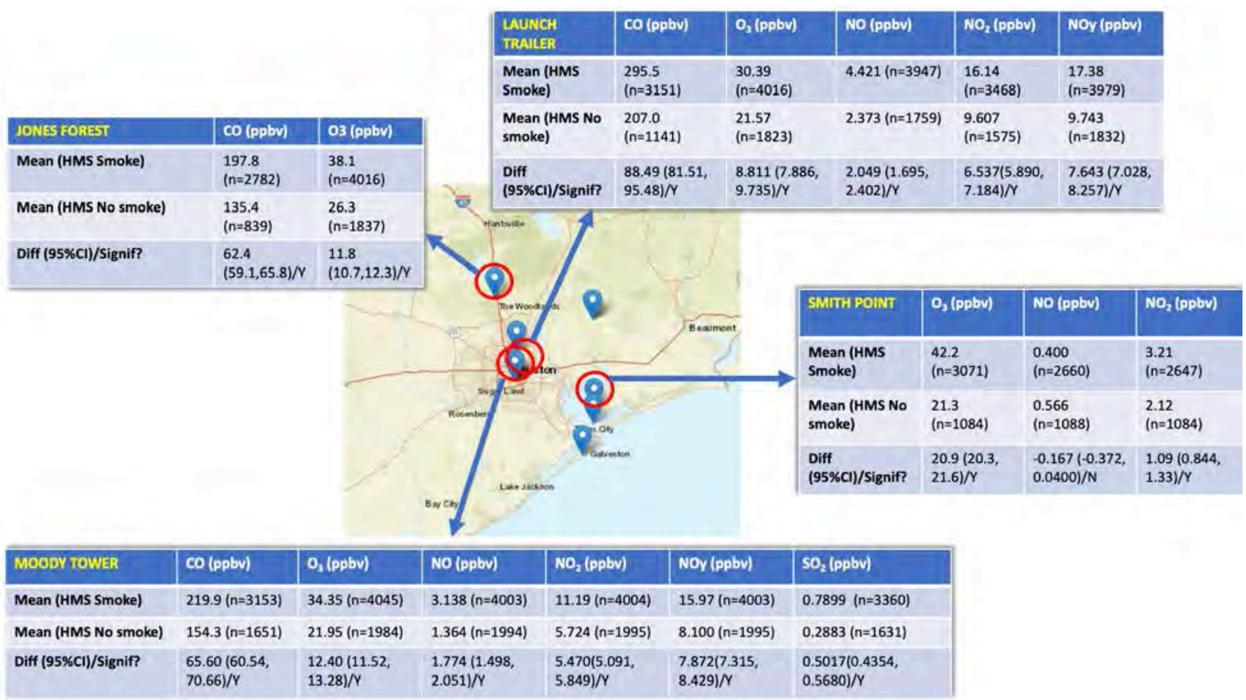

LAUNCH TRAILER	CO (ppbv)	O_3 (ppbv)	NO (ppbv)	NO_2 (ppbv)	NOy (ppbv)
Mean (HMS Smoke)	295.5 (n=3151)	30.39 (n=4016)	4.421 (n=3947)	16.14 (n=3468)	17.38 (n=3979)
Mean (HMS No smoke)	207.0 (n=1141)	21.57 (n=1823)	2.373 (n=1759)	9.607 (n=1575)	9.743 (n=1832)
Diff (95%CI)/Signif?	88.49 (81.51, 95.48)/Y	8.811 (7.886, 9.735)/Y	2.049 (1.695, 2.402)/Y	6.537(5.890, 7.184)/Y	7.643 (7.028, 8.257)/Y

JONES FOREST	CO (ppbv)	O3 (ppbv)
Mean (HMS Smoke)	197.8 (n=2782)	38.1 (n=4016)
Mean (HMS No smoke)	135.4 (n=839)	26.3 (n=1837)
Diff (95%CI)/Signif?	62.4 (59.1,65.8)/Y	11.8 (10.7,12.3)/Y

SMITH POINT	O_3 (ppbv)	NO (ppbv)	NO_2 (ppbv)
Mean (HMS Smoke)	42.2 (n=3071)	0.400 (n=2660)	3.21 (n=2647)
Mean (HMS No smoke)	21.3 (n=1084)	0.566 (n=1088)	2.12 (n=1084)
Diff (95%CI)/Signif?	20.9 (20.3, 21.6)/Y	-0.167 (-0.372, 0.0400)/N	1.09 (0.844, 1.33)/Y

MOODY TOWER	CO (ppbv)	O_3 (ppbv)	NO (ppbv)	NO_2 (ppbv)	NOy (ppbv)	SO_2 (ppbv)
Mean (HMS Smoke)	219.9 (n=3153)	34.35 (n=4045)	3.138 (n=4003)	11.19 (n=4004)	15.97 (n=4003)	0.7899 (n=3360)
Mean (HMS No smoke)	154.3 (n=1651)	21.95 (n=1984)	1.364 (n=1994)	5.724 (n=1995)	8.100 (n=1995)	0.2883 (n=1631)
Diff (95%CI)/Signif?	65.60 (60.54, 70.66)/Y	12.40 (11.52, 13.28)/Y	1.774 (1.498, 2.051)/Y	5.470(5.091, 5.849)/Y	7.872(7.315, 8.429)/Y	0.5017(0.4354, 0.5680)/Y

Figure 1. Map of selected surface air quality monitoring sites in HGB. Tables show concentrations of species measured at each circled site, divided into HMS-smoke and HMS-no smoke categories.

After identifying fire locations, HMS analysts use imagery from multiple NOAA and NASA satellites to identify the geographic extent of smoke plumes (Rolph et al., 2009; Ruminski et al., 2006). Due to the frequent interference by cloud cover, the number and extent of smoke plumes reported in the HMS represents a conservative estimate.

In addition to the HMS, we use the Fire Inventory from NCAR (FINN v2.5, Wiedinmyer et al., 2011, McDonald-Buller et al., 2015) to determine fire counts within different distances from the city center (0.5, 1.0, 2.5, 5.0, 10.0, and 25.0 degrees (lat/lon) from the city).

We also convolved the FINN 0.1-degree estimates of total NO_x, volatile organic compounds (VOC), and $PM_{2.5}$ emissions from fires with daily estimates of upwind influences on HGB and El Paso measurements (i.e., upwind surface "footprints" calculated from STILT) to determine the daily transport of O_3 precursors and primary $PM_{2.5}$ to each city. The Stochastic Time-Inverted Lagrangian Transport (STILT) model (Lin et al., 2003; Nehrkorn et al., 2010) is an enhanced version of the HYSPLIT model (Draxler and Hess, 1998) aimed at mass conservation, a critical consideration for inversion work. STILT computes the "footprint" (adjoint of the transport field) by following an ensemble of tracer particles backwards in time from the location of each measurement ("receptor"). The footprint (units: ppm/μmol m^{-2} s^{-1}) quantifies the concentration enhancement at the receptor at each point in time due to unit surface flux at each upwind location. Here we will generate daily STILT footprints for each urban area driven with 12 km NAM meteorological data. As with the HYSPLIT predictors in Section 1.2.1.2, these footprints will be initialized at local noon at a height of 300 m and will go at least 72 hours back in time.

Note that, as STILT does not account for the chemistry along the transport path, it cannot directly account for the chemical formation of O_3 and $PM_{2.5}$ as the smoke is transported from the fire. Instead, we will use the STILT footprints multiplied by the FINN fire emissions as an indicator of smoke transport and see how this smoke indicator correlates with O_3 and $PM_{2.5}$. We will also examine how the predictions depend on smoke age by segregating the footprint predictors into fresh smoke (< 24 hours transport time from fire to city) and aged smoke (≥ 24 hours).

Here we test several fire and smoke predictors based on the HMS and FINN data, including:

a. A binary predictor for the presence of smoke according to the NOAA HMS (Figure 1)
b. The total FINN fire counts in surrounding regions binned by distance from the city at 0.5, 1.0, 2.5, 5.0, 10.0, and 25.0 degrees (lat/lon).
c. FINN fire counts and total emissions for different geographic regions: Yucatan, all of Mexico, California, and states bordering Texas (LA, AR, OK, NM).
d. WRF-STILT footprints for NO, NO_2, CO_2, and CO.

2.4 CAMx Data

TCEQ generated CAMx output for the Houston (4 km horizontal resolution) and El Paso (12 km resolution) for the year 2019 was used for the comparison with observed data. MDA8 O_3 values were calculated for each monitoring location based on the CAMx grid box that contained the monitoring location. New CAMx-based values for the maximum MDA8 O_3 and background MDA8 O_3 value for each urban area by date were calculated using the same methods used for the ambient data (Section 2.1). These were added to the model training dataset with a new flag, "Is_Model", which is 1 for data from CAMx and 0 for ambient data. All other parameters were kept identical for the "Is_Model" cases, such that the new lines only differ from the ambient data in their values for Max MDA8 O_3, background MDA8 O_3, and Is_Model.

3 Generalized Additive Models

GAMs are a form of linear modeling which allows non-linear functions of individual predictors within a regression framework (Wood, 2017). This is like standard linear regression techniques, which optimize scalar coefficients (a_k) for each predictor (x_k) for k = 1 to p:

$$\hat{y} = \alpha_0 + \alpha_1 x_1 + \alpha_2 x_2 + \ldots + \alpha_p x_p$$

except that the coefficients are replaced with potentially non-linear smooth functions:

$$\hat{y} = s_0 + s_1(x_1) + s_2(x_2) + \ldots + s_p(x_p)$$

The GAM approach optimizes these smooth functions. An advantage of GAMs over neural networks and similar machine learning techniques is that it is easy to isolate the effects of the individual variables in GAMs. This will allow us to separate the impact of fire-related variables from the impact of the rest of the predictors. A potential disadvantage relative to standard linear regression is that the smooth functions can overfit the data, and so care needs to be taken to ensure that the derived smooth functions are realistic and robust to changes in the training data set. To address this, the R package mgcv includes routines to fit GAMs, examine the models graphically, and test their robustness via k-fold cross-validation and other techniques.

In this study, all meteorological predictors and the FINN fire counts were simulated as smooth functions using cubic spline basis set, with periodic splines used to account for the effects of the day of year and HYSPLIT bearing. Year, day of week, and the HMS smoke flag were included as factor variables. The models predict the natural logarithm of O_3 and $PM_{2.5}$ concentrations as these are usually log-normally distributed.

4 Results

4.1 Objective 1: Impact of fires on urban AQ in Texas

4.1.1 Smoke Flag Tests

In these tests, we trained GAMs by adding the HMS smoke flag to the meteorological predictors listed in Section 2.2. For ozone, the HMS smoke flag was always a significant predictor ($p<0.001$). All predictors included were highly significant ($p<0.001$) in Houston, while in El Paso they were all highly significant except for afternoon mean temperature, which was still very significant ($p<0.02$). Table 2 summarizes the change in the quality of the model fits with and without the smoke flags by examining the deviance explained, the total model degrees of freedom, and the Akaike information criterion (AIC). A lower AIC indicates a better model fit. In all cases, adding the HMS smoke flag leads to a slightly better model fit while the increase in degrees of freedom for the model is less than 1.

Table 2. Degrees of freedom (df), Akaike information criterion (AIC), and deviance explained (Dev. Exp., %) for each ozone model.

	With Smoke Flag			**Without Smoke Flag**		
	df	AIC	Dev. Exp.	df	AIC	Dev. Exp.
Houston Bkgrd	46.9	16353	63.7%	46.2	16445	63.4%
Houston Max	46.5	17129	67.2%	45.9	17224	67.0%
El Paso Bkgrd	44.2	15350	51.5%	43.4	15429	51.0%
El Paso Max	43.1	15696	54.2%	42.2	15764	53.9%

With these models, we then estimate the impact of smoke on background and maximum MDA8 O_3 in each urban area by calculating the GAM predictions with the true smoke flag minus the GAM predictions when the smoke flag is set to 0 for all days. We calculated this difference for all days where the HMS indicated smoke over the city (~10% of days). The distributions of these smoke-related differences are summarized in Table 3. We see similar mean impacts on background MDA8 O_3 in each urban area (2.4 ppbv). However, in Houston we see a slight increase in MDA8 O_3 (0.2 ppbv) in the city on smoky days, while in El Paso we see a slight decrease (0.5 ppbv). This suggests that in city chemistry has little impact on the ozone impacts from smoke and can either increase or decrease those impacts. Note that while these tests only account for the presence of smoke as indicated by HMS, not its concentration, we can conclude that the presence of smoke over the city as indicated by HMS is associated with an increase in MDA8 O_3 that can vary from 1.2 ppbv to 4.8 ppbv, and thus the HMS smoke product can be treated as significant evidence that the MDA8 O_3 for a given day was increased by smoke.

Table 3. Change in MDA8 O_3 due to the presence of smoke as indicated by the HMS smoke flag in the GAMs trained only on the meteorological predictors and the HMS smoke flag.

	Houston MDA8 O_3		**El Paso MDA8 O_3**	
	Bkgrd (ppbv)	Max (ppbv)	Bkgrd (ppbv)	Max (ppbv)
Minimum	1.2	1.5	1.7	1.4
25th Percentile	1.9	2.1	2.2	1.8
Median	2.3	2.5	2.4	1.9
Mean	2.4	2.6	2.4	1.9
75th percentile	2.8	3.0	2.5	2.0
Max	4.7	4.8	2.9	2.4
Std. Dev.	0.64	0.60	0.23	0.19

Unfortunately, the $PM_{2.5}$ GAM fits, both with and without the smoke flag, showed very poor performance. The total deviance explained generally less than 30%, and the residual plots versus fitted values (not shown) indicated significant heteroskedacity in the data. Several variable transformations were attempted to resolve this issue, but not removed the heteroskedacity. Simple correlation analysis also suggested that further attempts were unlikely to succeed, as the predictor variables have very low correlations with either background or maximum $PM_{2.5}$.

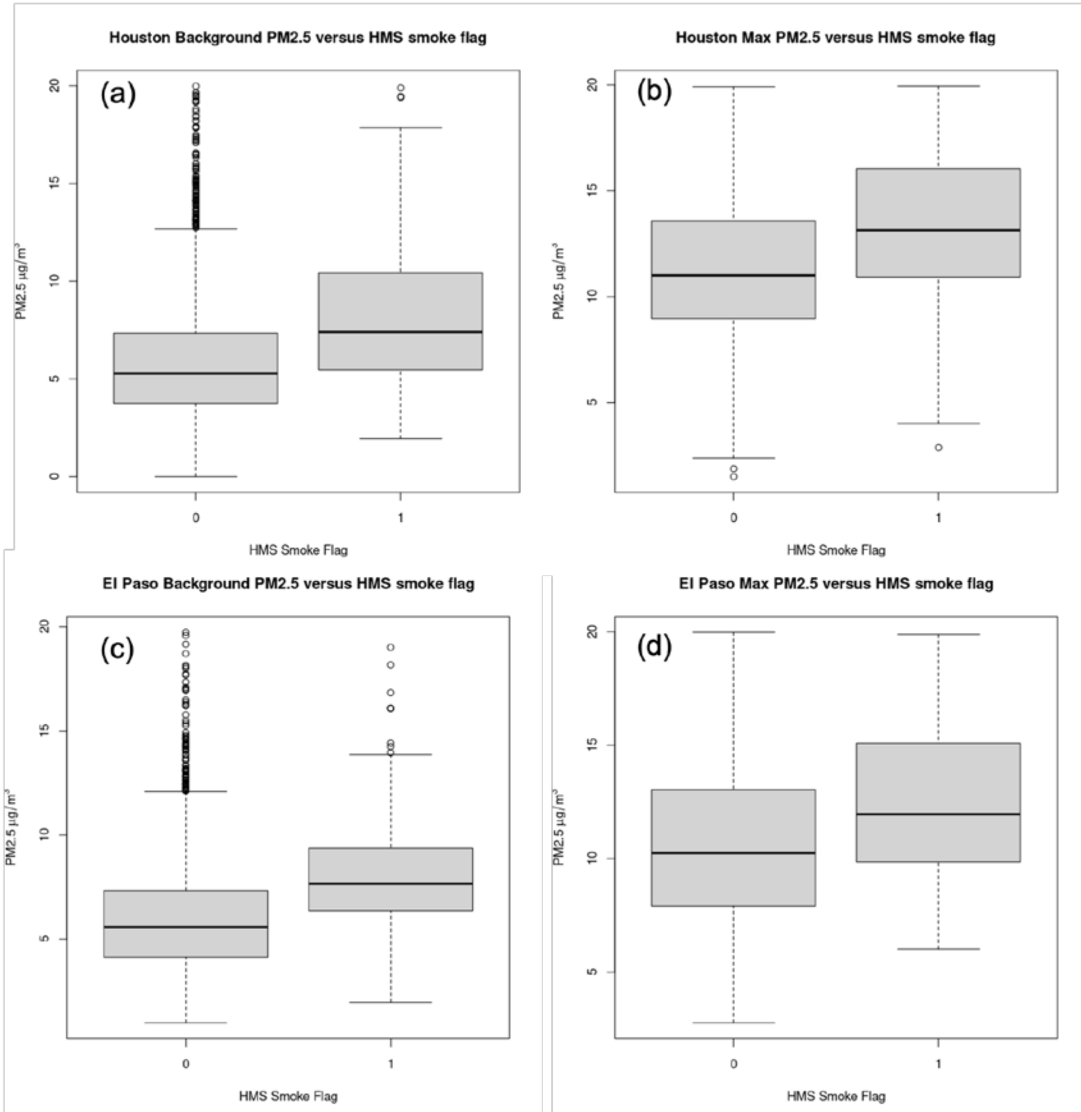

Figure 2. Box and whisker plots pf the daily average $PM_{2.5}$ differences on days with the HMS indicating smoke overhead (smoke flag = 1) and with no smoke overhead (smoke flag = 0). (a) Houston background $PM_{2.5}$. (b) Houston maximum $PM_{2.5}$. (c) El Paso background $PM_{2.5}$. (d) El Paso Maximum $PM_{2.5}$.

Thus, instead of showing GAM fit results that are unreliable, we used the simpler approach of comparing the distributions of maximum and background $PM_{2.5}$ for days with and without HMS smoke. Figure 2 shows box plots for the four cases. In all cases, the $PM_{2.5}$ distributions on days where HMS indicated smoke have higher mean $PM_{2.5}$ concentration, and the differences in the means (t-test) and the distributions (Kolmorogov-Smirnov test) are statistically significant at $p << 0.001$. The 95% confidence intervals of the mean differences are:

- Houston $PM_{2.5}$ Background: 1.9-2.6 µg/m^3
- Houston $PM_{2.5}$ Max: 1.5-2.3 µg/m^3
- El Paso $PM_{2.5}$ Background: 1.7-2.5 µg/m^3
- El Paso $PM_{2.5}$ Max: 1.5-2.6 µg/m^3

This suggests that on average, days where the HMS indicated smoke overhead have about 2 $\mu g/m^3$ more $PM_{2.5}$ at the surface, but that these differences to not significantly change between the background and the city core, so the urban chemistry has little impact on the $PM_{2.5}$ impact of fires.

4.1.2 FINN fire count tests

We then added the different FINN fire count bins to our O_3 GAMs without the HMS smoke flag to determine which count distance improved the fit the most. The different predictors were evaluated using the deviance explained by the GAM, the minimized generalized cross-validation (GCV) score, and the statistical significance of the predictor in the fit. The results for background O_3 are shown in Table 4 and the results for maximum O_3 are in Table 5. For El Paso, the best results are for using a ±25 degree (lat/lon) box around the city to calculate fire counts. This area includes the Yucatan peninsula and California, major locations of annual fires. The Houston maximum O_3 is best fit with a ±10-degrees box, which includes the Yucatan. For Houston background O_3, the ±5-degree box is slightly better, but to keep consistency with the maximum we choose to use the 10-degree box. In all cases, adding the smoke flag to the chosen FINN fire count predictor increases the quality of the fit. Thus, we examine the fire impacts on ozone implied by the GAMs using (a) the meteorological predictors from Section 2.2, (b) the HMS smoke flag, and (c) the FINN fires counts at ±10-degrees from Houston and ±25-degrees from El Paso. This suggests that the impact of smoke is primarily from remote fires (1000 to 2500 km away).

Table 4. Quality of fit for GAMs using different FINN fire count predictors to predict maximum MDA8 O_3.

	Houston Max MDA8 O_3			El Paso Max MDA8 O_3		
	Dev. Exp. (%)	GCV	p	Dev. Exp. (%)	GCV	p
0.5 degrees	67.5	83.019	<0.001	53.9	46.927	0.75
1.0 degrees	67.7	82.492	<0.001	53.9	46.899	0.21
2.5 degrees	68.4	80.655	<0.001	54.1	46.741	<0.01
5.0 degrees	68.7	79.895	<0.001	54.2	46.608	<0.001
10 degrees	***69.0***	***79.214***	***<0.001***	54.1	46.859	0.08
25 degrees	67.5	82.795	<0.001	***54.9***	***45.988***	***<0.001***
Best + HMS smoke flag	**69.1**	**79.025**	**<0.001**	**55.1**	**45.959**	**<0.001**

Table 5. Quality of fit for GAMs using different FINN fire count predictors to predict background MDA8 O_3.

	Houston Bkgrd MDA8 O_3			El Paso Bkgrd MDA8 O_3		
	Dev. Exp. (%)	GCV	p	Dev. Exp. (%)	GCV	p
0.5 degrees	63.5	60.402	0.05	51.0	40.737	0.76
1.0 degrees	63.7	60.14	0.001	51.0	40.739	0.69
2.5 degrees	64.1	59.389	<0.001	51.2	40.619	0.01
5.0 degrees	***64.4***	***58.959***	***<0.001***	51.2	40.621	0.04
10 degrees	64.4	59.072	<0.001	51.3	40.619	0.01
25 degrees	64.0	59.671	<0.001	***52.3***	***39.788***	***<0.001***
Best + HMS smoke flag	**64.6**	**58.890**	**<0.001**	**52.6**	**39.641**	**<0.001**

As in Section 4.1.1, we use the GAMs to calculate the MDA8 O_3 first using the actual HMS smoke flag and FINN fire counts, and then estimate a smoke-free case by setting the smoke flag to 0 for all days and setting the FINN fire count variables to their minimums on smoky days (30 for the ±10-degree Houston box and 400 for the ±25-degree El Paso box). The distribution of these differences on days where the HMS indicated smoke overhead are shown in Table 6. In general, these more advanced GAMs indicate a larger influence of smoke on background MDA8 O_3 in these urban areas that the smoke flag only GAMs did, averaging 6.1 ppbv in El Paso and 7.8 ppbv in Houston. In addition, while the El Paso differences between the background and maximum impacts of smoke follow the previous pattern of a decrease as the smoke enters the city (-1.6 ppbv on average), in Houston we now see a significant increase related to the fire predictors (+6.0 ppbv). These differences in smoke impact between the background and maximum MDA8 O3 are statistically significant at $p<<0.001$ (t-test and Kolmorogov-Smirnov test). It is unclear why these urban areas have such significant differences in the estimated smoke impact on urban chemistry. The decrease in El Paso could be due to NO titration of the O_3 from the fires, while the Houston results would suggest a significant impact of the fire-related VOCs on the urban chemistry.

Table 6. Change in MDA8 O_3 due to the presence of smoke as indicated by the HMS smoke flag in the GAMs trained on the meteorological predictors, the HMS smoke flag, and FINN fire counts.

	Houston MDA8 O_3		**El Paso MDA8 O_3**	
	Bkgrd (ppbv)	Max (ppbv)	Bkgrd (ppbv)	Max (ppbv)
Minimum	1.3	2.4	2.7	1.9
25th Percentile	5.8	11.3	5.3	3.3
Median	7.9	13.6	6.1	4.3
Mean	7.8	13.8	6.1	4.5
75th percentile	9.6	16.9	6.9	5.7
Max	18.4	28.2	9.4	8.8
Std. Dev.	3.0	4.3	1.4	1.4

4.1.3 Geographic FINN fire count and emissions fits

To further investigate the influence of fire emissions on urban MDA8 O_3 in Houston and El Paso, we calculated total fire counts and emissions of multiple species in geographic regions near Texas: the Yucatan (YUC), all of Mexico (MEX), California (CA), and states bordering Texas (LA, AR, OK, NM). We then replaced the FINN fire count predictors used in Section 4.1.2 above with these new predictors one by one to find the FINN variable in each region that gave the best fit with MDA8 background and maximum O_3. The best variables for each region and predictand are given in Table 7.

Table 7. Best FINN fire variable by geographic region.

	Houston		El Paso	
Region	Maximum MDA8 O_3	Background MDA8 O_3	Maximum MDA8 O_3	Background MDA8 O_3
MEX	Biomass burned (BMASS)	Non-methane hydrocarbon (NMHC) emissions	BMASS	Xylene emissions
YUC	Fire Area	Fire Count	Fire Area	Fire Area
OK	Fire Count	BMASS	Fire Count	Fire Count
NM	Fire Count	Fire Count	Fire Count	Fire Count
LA	Fire Count	Fire Count	Hydroxyacetone (HYAC) emissions	CH_3CN emissions
AR	Fire Count	NMHC emissions	Fire Count	Fire Count
CA	NO_x emissions as NO	Glycoladehyde (GLYALD) emissions	NO_x emissions as NO	Fire Area

The general FINN fire count predictors used in Section 4.1.2 were replaced with these geographic variables and the GAMs were rerun. Variables that were not significant at least $p < 0.10$ were removed and the fits rerun. The results were:

- Houston Max O_3 – Only MEX, AR, and NM kept as significant predictors. Total deviance explained was 68.2% with a GCV of 81.6, which is a better fit than the large-scale FINN fire count fit from Section 4.1.2. Increases in Mexican biomass burned and Arkansas fire counts were associated with increased O_3 but saturated at relatively low values, while NM fire counts slightly decreased O_3 (Figure 3).

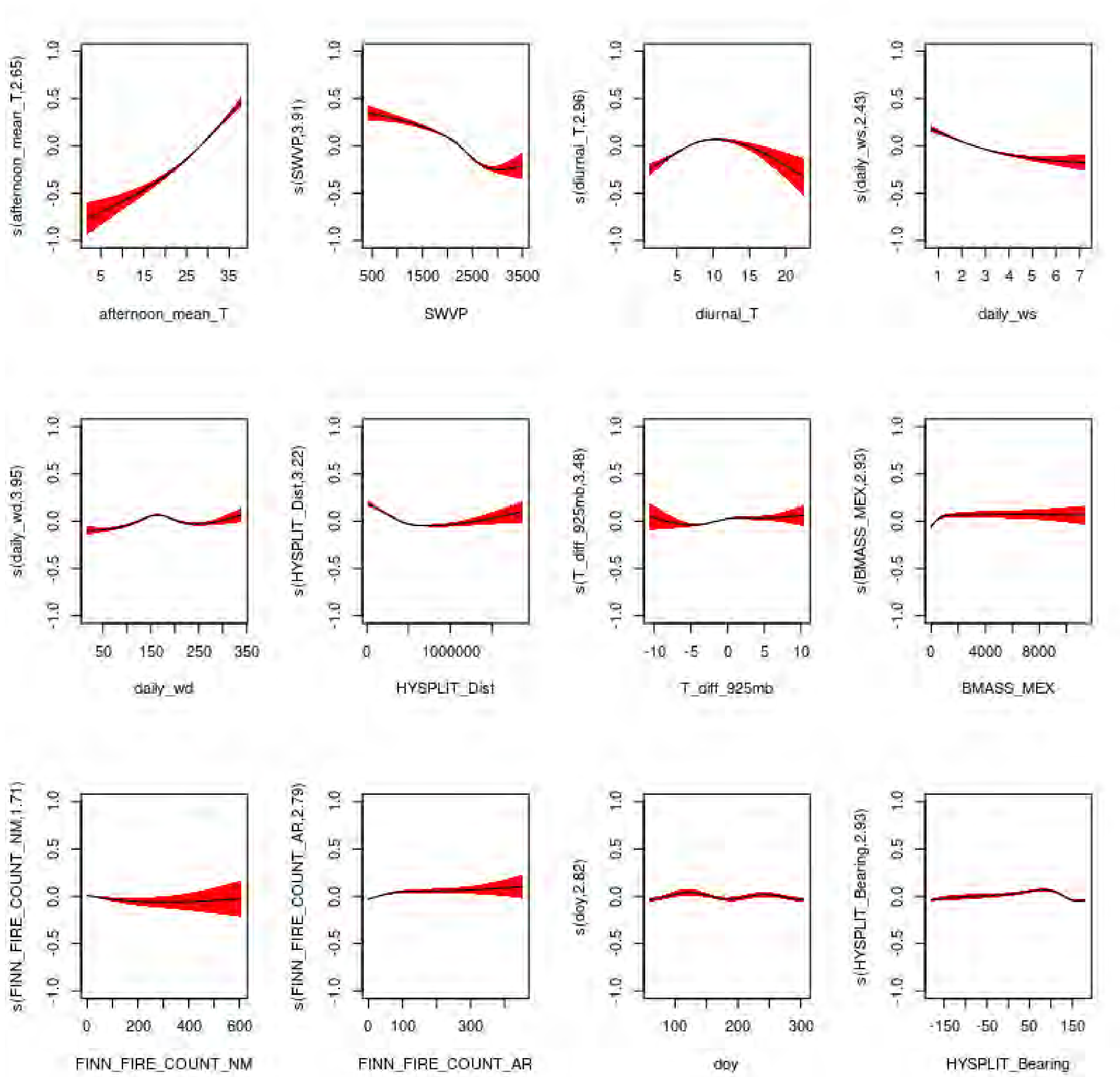

Figure 3. Smooth function fits for the log of maximum MDA8 O_3 in Houston.

- Houston Background O_3 – All variables were kept as significant predictors. Total deviance explained was 65.5% with a GCV of 57.9, which is a better fit than the large-scale FINN fire count fit from Section 4.1.2. All fire impacts were positive except for NM, with MEX and AR showing the largest impacts (Figure 4).

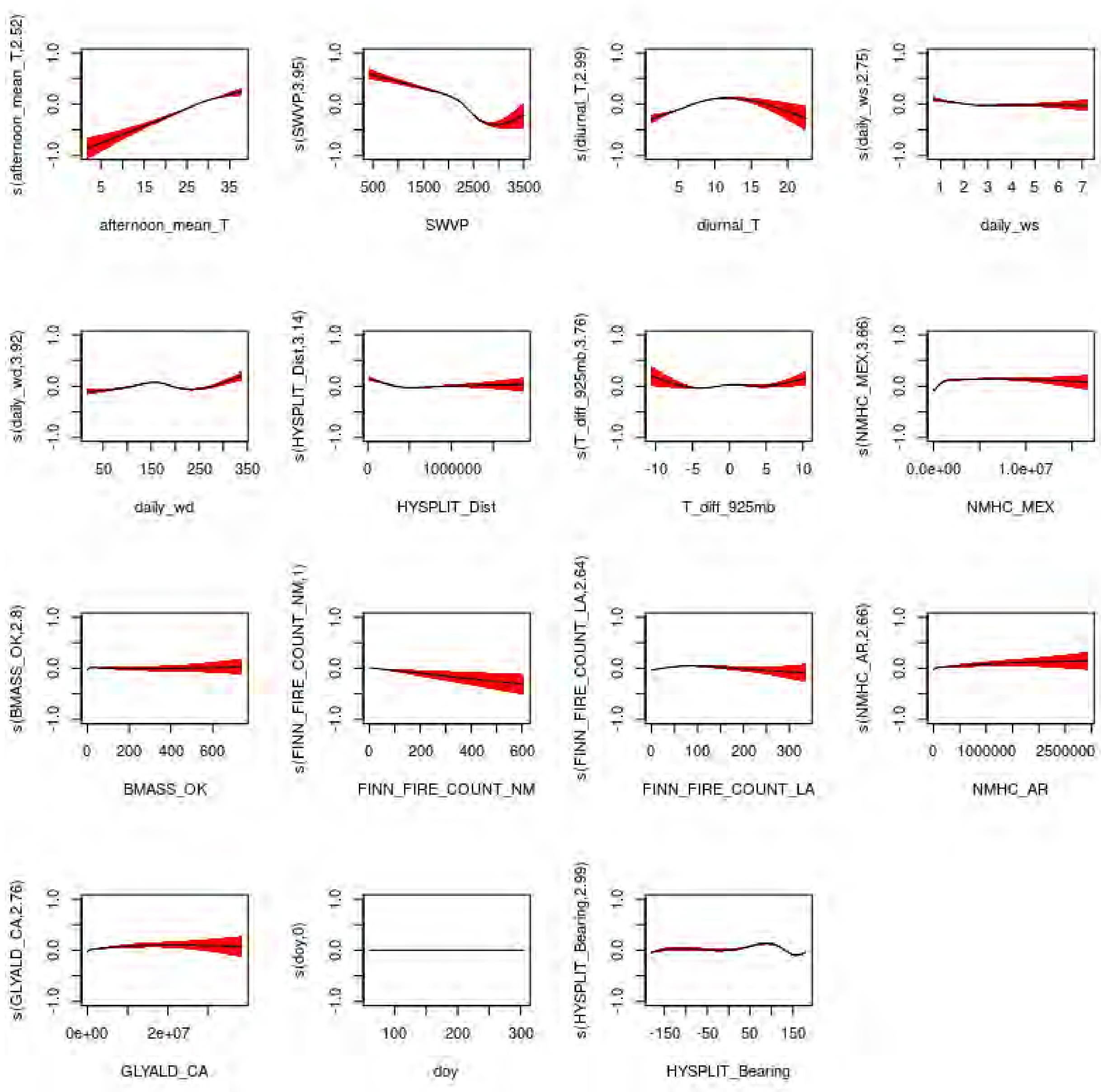

Figure 4. Smooth function fits for the log of background MDA8 O_3 in Houston.

- El Paso Max O_3 – AR was removed, but all other variables kept as significant predictors. Total deviance explained was 57.1% with a GCV of 44.43, which is a better fit than the large-scale FINN fire count fit from Section 4.1.2. Only the Mexico predictor had a large increase in O_3 and saturated quickly (Figure 5).

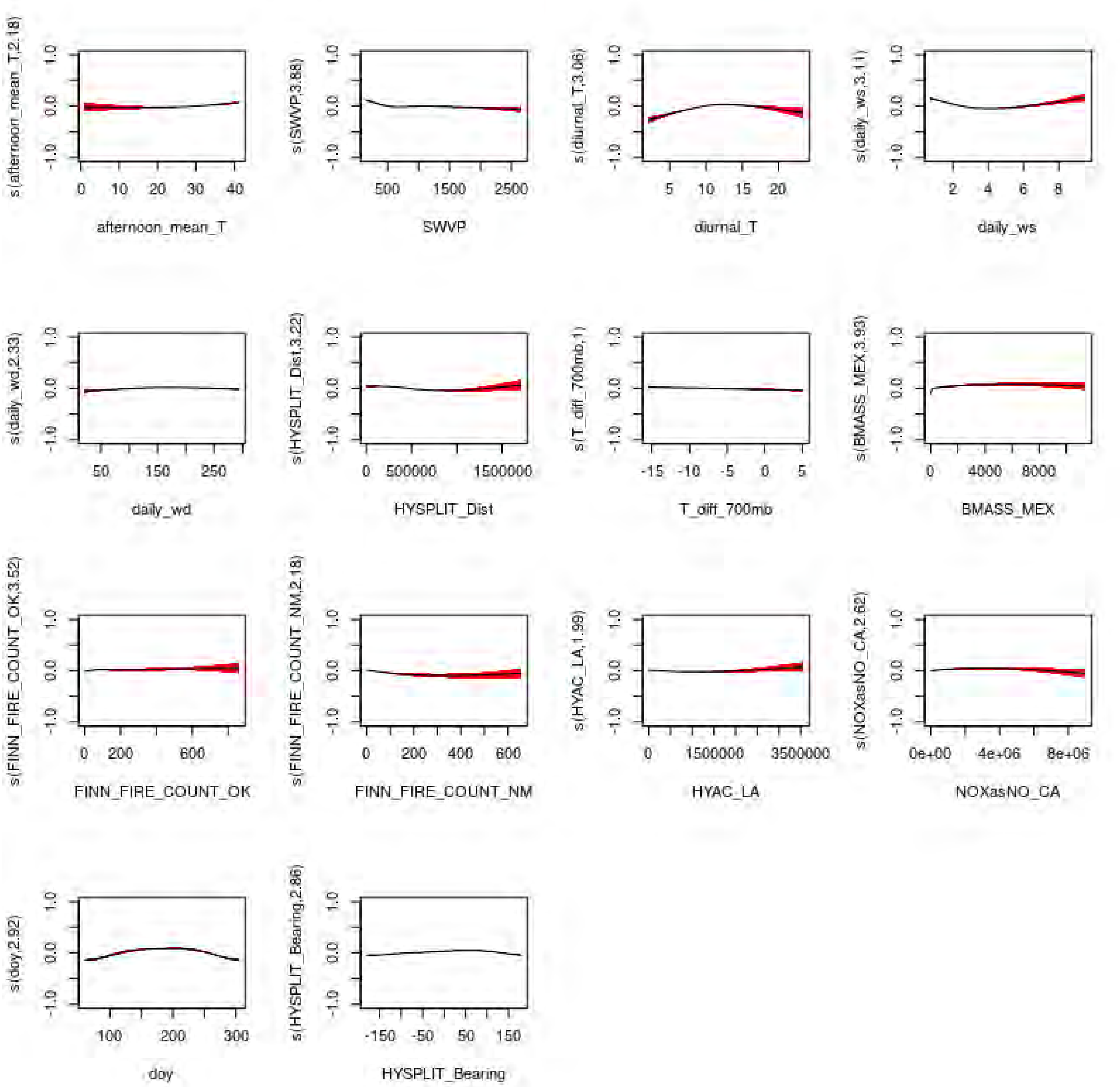

Figure 5. Smooth function fits for the log of maximum MDA8 O_3 in El Paso.

- El Paso Background O_3 – AR was removed, but all other variables kept as significant predictors. Total deviance explained was 54.4% with a GCV of 38.57, which is a better fit than the large-scale FINN fire count fit from Section 4.1.2. Mexico tended to increase O_3 while NM decreased it (Figure 6).

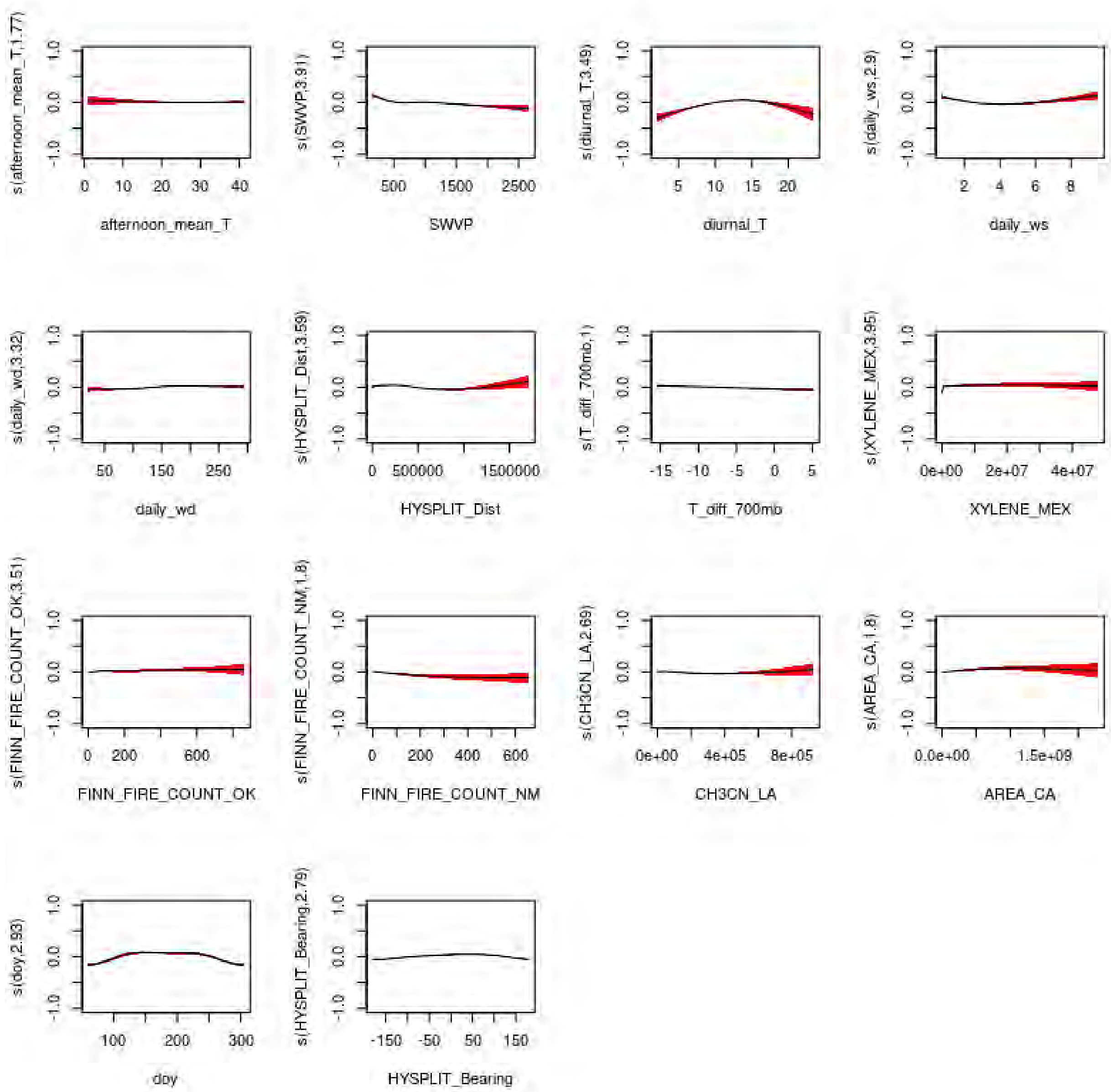

Figure 6. Smooth function fits for the log of background MDA8 O_3 in El Paso.

As before, we use the GAMs to calculate the MDA8 O_3 first using the actual HMS smoke flag and geographic FINN variables, and then estimate a smoke-free case by setting the smoke flag to 0 for all days and setting the geographic FINN variables to their minimums on smoky days. The distribution of these differences on days where the HMS indicated smoke overhead are shown in Table 8. In this case, the GAMs predict relatively large impacts of smoke on background and maximum MDA8 O_3 in both urban areas (means of 7-8 ppbv) with a slight decrease in the smoke related O_3 when the smoke enters the city (-0.9 ppbv mean for Houston, -0.2 ppbv mean for El Paso). The small changes as the smoke enters the city are similar to the smoke flag only results from Section 4.1.1, but the absolute impact of smoke is estimated to be much higher in this fit.

Table 8. Change in MDA8 O_3 due to the presence of smoke as indicated by the HMS smoke flag in the GAMs trained on the meteorological predictors, the HMS smoke flag, and FINN geographic variables.

	Houston MDA8 O_3		**El Paso MDA8 O_3**	
	Bkgrd (ppbv)	Max (ppbv)	Bkgrd (ppbv)	Max (ppbv)
Minimum	1.0	2.0	1.6	0.3
25th Percentile	5.6	5.3	5.5	5.4
Median	7.7	7.0	7.4	7.2
Mean	8.0	7.1	7.2	7.0
75th percentile	9.8	8.4	8.7	8.5
Max	23.2	20.5	13.0	12.6
Std. Dev.	3.7	2.8	2.1	2.3

While the geographic FINN fits seem to have the best fitting statistics (deviance explained and GCV), the fact that they predict negative impacts for some areas suggests that they may be fitting significant amounts of noise. In addition, as the variables are not kept constant between the max and background fits, it is not clear if the deltas calculated for smoke entering the city are trustworthy.

4.1.4 WRF-STILT footprint fits

The convolved WRF-STILT footprints with the FINN emissions at 0.01x0.01 degrees generally gave similar fits regardless of the specific species fit. Thus, here we focus on the results for FINN NO. The convolved footprints were highly significant predictors ($p << 0.001$) of background and maximum MDA8 O_3 in Houston, but surprisingly were not significant predictors for El Paso. The deviance explained and GCV statistics for each fit were:

- Houston Maximum – Deviance explained 67.9%, GCV 81.9
- Houston Background – Deviance explained 64.2%, GCV 59.4
- El Paso Maximum – Deviance explained 54.2%, GCV 46.1
- El Paso Background – Deviance explained 51.8%, GCV 39.8

These fit statistics are generally worse than those using the FINN fire count variables directly in Sections 4.1.2 and 4.1.3, suggesting that the WRF-STILT footprints may not correctly represent the transport of biomass burning emissions to these urban areas.

As before, we use the GAMs to calculate the MDA8 O_3 first using the actual HMS smoke flag and NO footprints, and then estimate a smoke-free case by setting the smoke flag to 0 for all days and setting the NO footprints to their minimums on smoky days. The distribution of these differences on days where the HMS indicated smoke overhead are shown in Table 9. As only the Houston results had the footprints as significant predictors, we focus on those. In this case, the GAMs predicted a mean impact of smoke on Houston background O_3 of 4.5 ppbv, increasing by 2.2 ppbv as the smoke entered the city.

Table 9. Change in MDA8 O_3 due to the presence of smoke as indicated by the HMS smoke flag in the GAMs trained on the meteorological predictors, the HMS smoke flag, and the WRF-STILT/FINN NO footprints.

	Houston MDA8 O_3		**El Paso MDA8 O_3**	
	Bkgrd (ppbv)	Max (ppbv)	Bkgrd (ppbv)	Max (ppbv)
Minimum	-2.9	1.2	1.6	1.2
25^{th} Percentile	3.4	5.4	2.3	1.7
Median	4.7	6.6	2.6	1.9
Mean	4.5	6.7	2.7	2.0
75^{th} percentile	5.8	8.3	3.1	2.1
Max	10.22	13.3	4.7	5.8
Std. Dev.	1.9	2.4	0.6	0.6

Table 10 summarizes the mean results for Objective 1. Unfortunately, the results depend strongly on which set of fire predictors is used. For Houston, the range of impacts of fires on mean background MDA8 O_3 is 2.4 to 8.0 ppbv, with the change in O_3 impact as the smoke enters the city varying from -0.9 ppbv to +6.0 ppbv, with three out of four methods predicting an increase in mean O3 as the smoke enters the city. In El Paso, the range of impacts of fires on mean background MDA8 O_3 is 2.4 to 7.2 ppbv, similar to Houston, with the change in mean O_3 impact as the smoke enters the city varying from -1.6 ppbv to -0.5 ppbv. The geographic fire variables from Sec. 4.1.3 give the best fitting statistics and predicts fire impacts of 7.0-8.0 ppbv in both urban areas, with a slight decrease in the impact when the smoke enters the city.

Table 10. Mean smoke impacts on background and maximum MDA8 O3 in each urban area for different sets of smoke predictors.

	Houston MDA8 O_3		**El Paso MDA8 O_3**	
	Bkgrd (ppbv)	Max (ppbv)	Bkgrd (ppbv)	Max (ppbv)
Smoke flag only (Sec. 4.1.1)	2.4	2.6	2.4	1.9
+ large-scale fire counts (Sec. 4.1.2)	7.8	13.8	6.1	4.5
+ geographic fire variables (Sec. 4.1.3)	8.0	7.1	7.2	7.0
+ WRF-STILT footprints (Sec. 4.1.4)	4.5	6.7	2.7	2.0

4.2 Objective 2: Ability of CAMx to simulate fire impacts

We used the updated dataset with the CAMx data (Section 2.4) to retrain the GAMs for maximum and background MDA8 O_3 for El Paso and Houston (total of four cases). The significance of the "Is_Model" factor variable was used to determine if the differences between the CAMx and ambient results were statistically significant. The model smooth functions and factor values were then examined for differences between the GAM trained with CAMx data and the ones without CAMx data, and the predicted impacts of smoke by each model were examined for differences.

4.2.1 El Paso Maximum MDA8 O_3

Our early work (Section 4.1.2) had shown that combining the HMS smoke flag and the 25 degree FINN fire counts gave the best results for the ambient data for El Paso Maximum MDA8 O_3 values, and so those parameters were reused here. The "Is_Model" variable was highly significant for this case ($p<0.001$), suggesting that the CAMx and ambient model results are significantly different. However, an examination of the smooth functions for each fit (Figure 7) shows very little difference between the smooth function fits for the cases with and without CAMx data, including for the dependence of maximum O_3 on the FINN fire counts. The parametric coefficient for HMS smoke flag also showed only small differences between the two GAMs (0.024 for ambient data only, 0.021 when CAMx data is added). These results tend to suggest that the difference between the CAMx predictions and the ambient data could be mostly explained by a constant fractional bias which is mostly accounted for by the Is_Model factor variable coefficient.

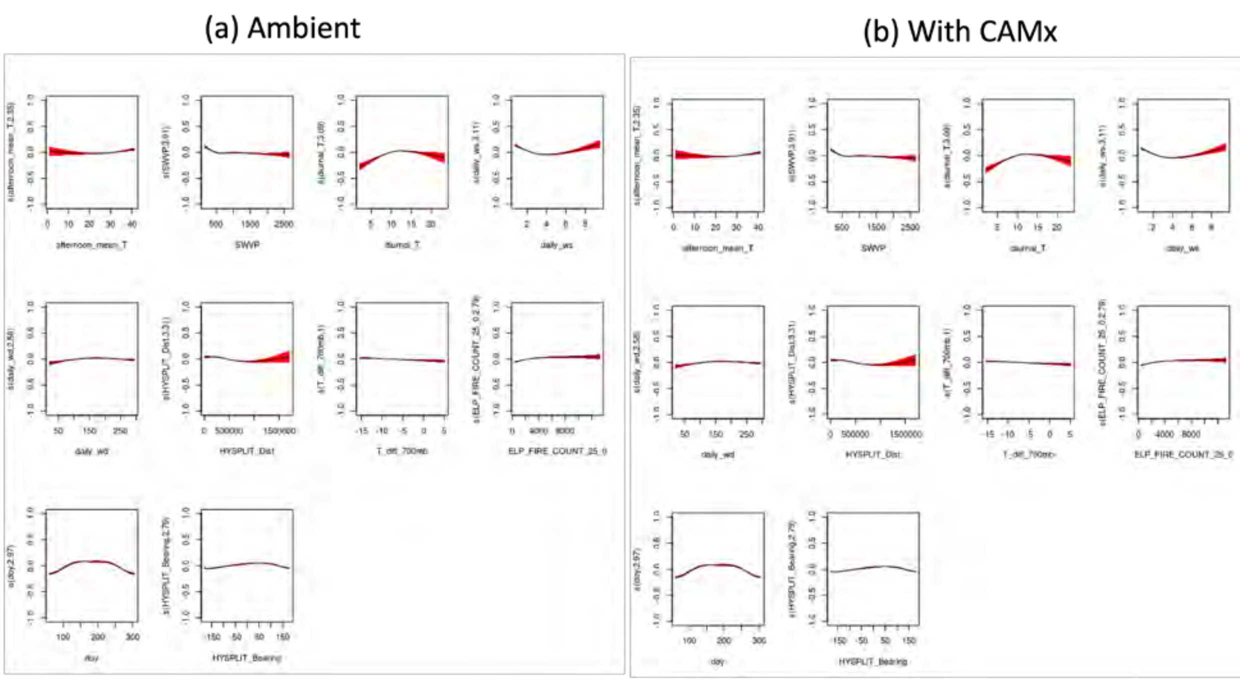

Figure 7. Smooth function fits for El Paso maximum MDA8 O_3 using (a) only ambient data and (b) using CAMx data with an Is_Model factor variable.

We further examined the differences by (a) comparing the maximum MDA8 O_3 predictions for 2019 for different values of the Is_Model variable to examine the fractional bias between the model and ambient data and (b) comparing the GAM predictions with and without the smoke variables for 2019 to examine how the predicted smoke impacts differ in the ambient data and the CAMx simulations. Table 11 shows the differences in the GAM predictions of the ambient and CAMx data for 2019. The mean percentage difference is -8% (i.e., CAMx underestimated the true mean by 8%), but the differences are larger for high O_3 days (-10%) than for low O_3 days (-3%), suggesting CAMx significantly underestimates the peak O_3 events in El Paso, leading to the significance of the Is_Model variable in the GAM fits.

Table 11. Ambient and CAMx GAM predictions for the 2019 maximum MDA8 O_3 (ppbv) for El Paso based on the GAM model with the Is_Model variable.

	Ambient (Is_Model = 0)	CAMx (Is_Model = 1)	% Difference
Minimum	35.3	34.1	-3%
25th Percentile	47.7	44.5	-7%
Median	53.4	49.7	-7%
Mean	52.7	48.7	-8%
75th percentile	57.8	53.1	-8%
Max	68.4	61.8	-10%
Std. Dev.	6.9	5.9	

Table 12 shows the difference in smoke impacts calculated for 2019 days where the HMS indicated smoke over El Paso. Note that this subset only includes 8 days. The GAMs trained on ambient data and the CAMx data make similar predictions for the fire impacts on these days, with the CAMx predictions generally being 0.3-0.4 ppbv smaller but showing no dependence with the strength of the ambient fire impact. This suggests that the CAMx predictions of MDA8 O_3 on fire days only slightly underpredict the actual impacts of fires on maximum MDA8 O_3 in El Paso.

Table 12. Estimated impact of smoke on the 2019 maximum MDA8 O_3 (ppbv) for El Paso when calculated from Ambient and CAMx data.

	Ambient	CAMx
Minimum	2.8	2.5
25th Percentile	4.0	3.7
Median	4.2	3.9
Mean	4.3	4.0
75th percentile	4.7	4.4
Max	5.6	5.2
Std. Dev.	0.8	0.8

4.2.2 El Paso Background MDA8 O_3

The “Is_Model” variable was highly significant for El Paso background O_3 ($p<0.001$), suggesting that the CAMx and ambient model results are significantly different. However, an examination of the smooth functions for each fit (Figure 8) shows very little difference between the smooth function fits for the cases with and without CAMx data, including for the dependence of maximum O_3 on the FINN fire counts. The parametric coefficient for HMS smoke flag also showed only small differences between the two GAMs (0.036 for ambient data only, 0.031 when CAMx data is added). These results tend to suggest that the difference between the CAMx predictions and the ambient data could be mostly explained by a fractional bias which is mostly accounted for by the Is_Model factor variable coefficient.

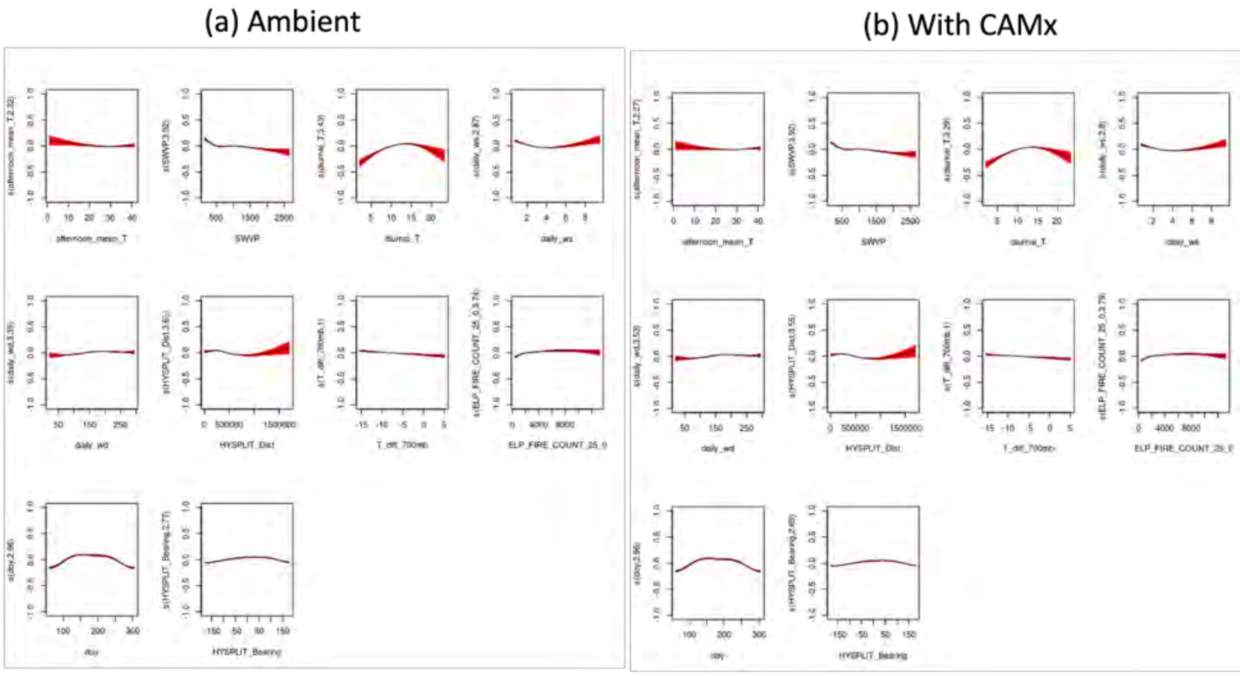

Figure 8. Smooth function fits for El Paso background MDA8 O_3 using (a) only ambient data and (b) using CAMx data with an Is_Model factor variable.

We further examined the differences by (a) comparing the maximum MDA8 O_3 predictions for 2019 for different values of the Is_Model variable to examine the fractional bias between the model and ambient data and (b) comparing the GAM predictions with and without the smoke variables for 2019 to examine how the predicted smoke impacts differ in the ambient data and the CAMx simulations. Table 13 shows the differences in the GAM predictions of the ambient and CAMx data for 2019. The mean percentage difference is -4% (i.e., CAMx underestimated the true mean by 4%), but the differences are generally larger for high O_3 days (-5%) than for low O_3 days (-1%).

Table 13. Ambient and CAMx GAM predictions for the 2019 background MDA8 O_3 (ppbv) for El Paso based on the GAM model with the Is_Model variable.

	Ambient (Is_Model = 0)	CAMx (Is_Model = 1)	% Difference
Minimum	33.7	32.1	-5%
25th Percentile	42.3	42.0	-1%
Median	48.2	46.2	-4%
Mean	47.6	45.9	-4%
75th percentile	52.5	50.6	-4%
Max	61.4	58.1	-5%
Std. Dev.	6.3	5.9	

Table 14 shows the difference in smoke impacts calculated for 2019 days where the HMS indicated smoke over El Paso. Note that this subset only includes 8 days. The GAMs trained on ambient data and the CAMx data make similar predictions for the fire impacts on these days, with the CAMx predictions generally being 0.2-0.4 ppbv smaller but showing no dependence with the strength of the ambient fire impact. This suggests that the CAMx predictions of MDA8 O_3 on fire days only slightly underpredict the actual impacts of fires on background MDA8 O_3 in El Paso.

Table 14. Estimated impact of smoke on the 2019 background MDA8 O_3 (ppbv) for El Paso when calculated from Ambient and CAMx data.

	Ambient	CAMx
Minimum	4.6	4.4
25th Percentile	6.3	6.0
Median	6.5	6.1
Mean	6.4	6.0
75th percentile	6.6	6.3
Max	7.6	7.2
Std. Dev.	0.8	0.8

4.2.3 Houston Maximum MDA8 O_3

Our previous work (Deliverable 2, Task 1) had shown that combining the HMS smoke flag and the 10 degree FINN fire counts gave the best results for the ambient data for Houston Maximum MDA8 O_3 values, and so those parameters were reused here. The "Is_Model" variable was **not** significant for this case ($p>>0.1$), suggesting that the CAMx and ambient model results are substantially the same. An examination of the smooth functions for each fit (Figure 9) shows very little difference between the smooth function fits for the cases with and without CAMx data, including for the dependence of maximum O_3 on the FINN fire counts. The parametric coefficient for HMS smoke flag also showed only small differences between the two GAMs (0.033 for ambient data only, 0.034 when CAMx data is added).

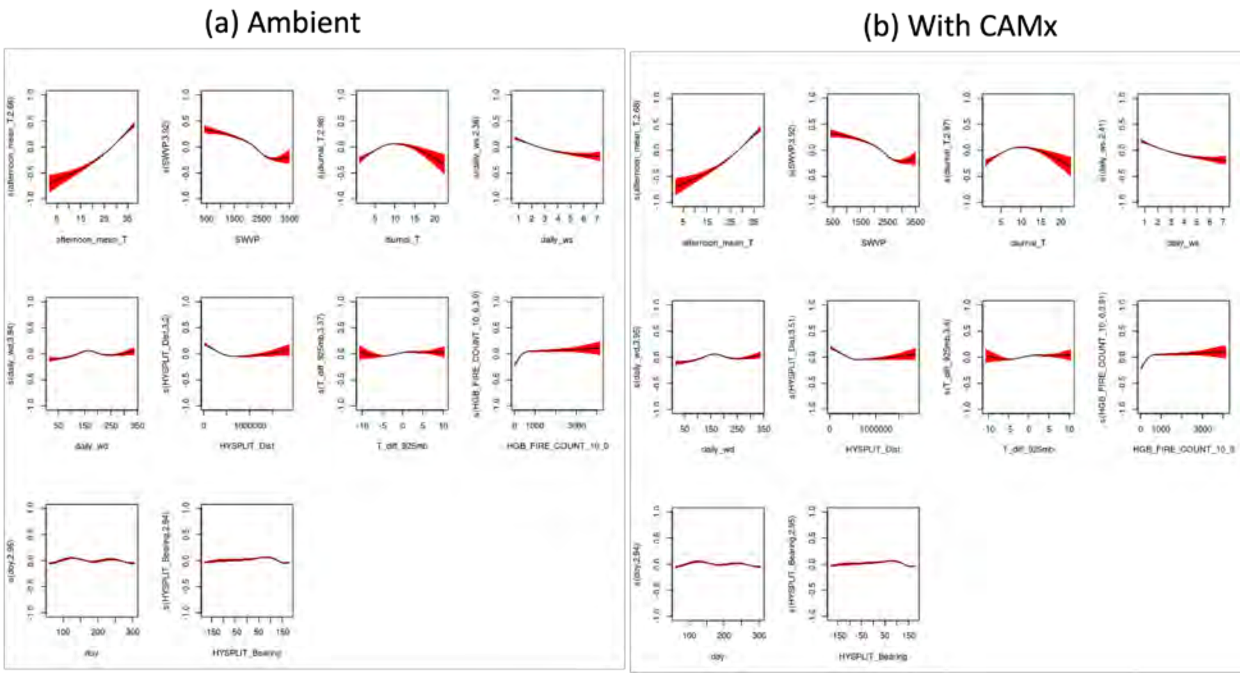

Figure 9. Smooth function fits for Houston maximum MDA8 O_3 using (a) only ambient data and (b) using CAMx data with an Is_Model factor variable.

We further examined the differences by (a) comparing the maximum MDA8 O_3 predictions for 2019 for different values of the Is_Model variable to examine the fractional bias between the model and ambient data and (b) comparing the GAM predictions with and without the smoke variables for 2019 to examine how the predicted smoke impacts differ in the ambient data and the CAMx simulations. Table 15 shows the differences in the GAM predictions of the ambient and CAMx data for 2019. The mean percentage difference is 3% (i.e., CAMx overestimated the true mean by 3%), but the differences are fairly constant with large changes in ambient O_3, consistent with the lack of significance for the Is_Model factor.

Table 15. Ambient and CAMx GAM predictions for the 2019 maximum MDA8 O_3 (ppbv) for Houston based on the GAM model with the Is_Model variable.

	Ambient (Is_Model = 0)	CAMx (Is_Model = 1)	% Difference
Minimum	27.7	28.2	2%
25^{th} Percentile	42.7	43.7	2%
Median	50.2	51.2	2%
Mean	52.4	53.9	3%
75^{th} percentile	61.3	62.5	2%
Max	82.9	84.1	1%
Std. Dev.	12.5	12.6	

Table 16 shows the difference in smoke impacts calculated for 2019 days where the HMS indicated smoke over Houston. Note that this subset only includes 35 days. The GAMs trained on ambient data and the CAMx data make similar predictions for the fire impacts on these days, with the CAMx predictions generally being 0.2-0.4 ppbv larger but showing no dependence with the strength of the ambient fire impact. This suggests that the CAMx predictions of MDA8 O_3 on fire days only slightly underpredict the actual impacts of fires on maximum MDA8 O_3 in Houston.

Table 16. Estimated impact of smoke on the 2019 maximum MDA8 O_3 (ppbv) for Houston when calculated from Ambient and CAMx data.

	Ambient	CAMx
Minimum	9.4	11.0
25th Percentile	12.7	12.9
Median	15.3	15.6
Mean	15.6	15.8
75th percentile	18.3	18.1
Max	21.5	21.8
Std. Dev.	3.4	3.3

4.2.4 Houston Background MDA8 O_3

The "Is_Model" variable was highly significant for Houston background O_3 ($p<0.001$), suggesting that the CAMx and ambient model results are significantly different. However, an examination of the smooth functions for each fit (Figure 10) shows very little difference between the smooth function fits for the cases with and without CAMx data, including for the dependence of maximum O_3 on the FINN fire counts. However, the parametric coefficient for HMS smoke flag is different between the two GAMs (0.058 for ambient data only, 0.063 when CAMx data is added).

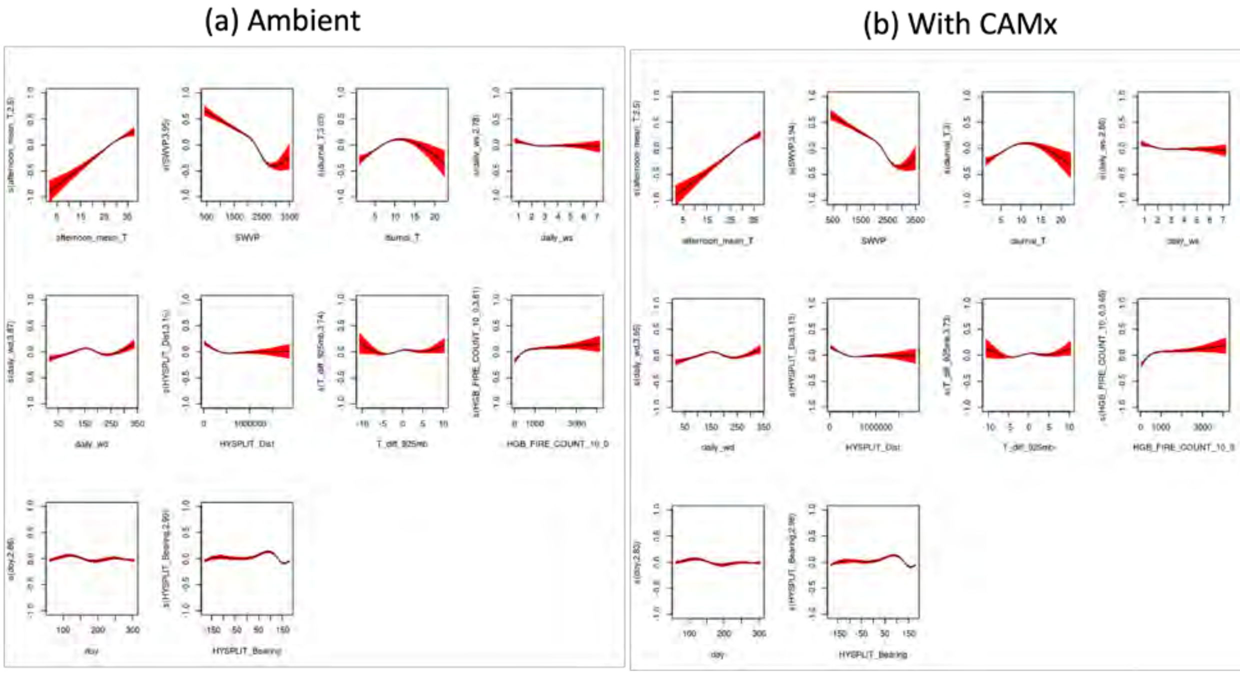

Figure 10. Smooth function fits for Houston background MDA8 O_3 using (a) only ambient data and (b) using CAMx data with an Is_Model factor variable.

We further examined the differences by (a) comparing the maximum MDA8 O_3 predictions for 2019 for different values of the Is_Model variable to examine the fractional bias between the model and ambient data and (b) comparing the GAM predictions with and without the smoke variables for 2019 to examine how the predicted smoke impacts differ in the ambient data and the CAMx simulations. Table 17 shows the differences in the GAM predictions of the ambient and CAMx data for 2019. The mean percentage difference is 21% (i.e., CAMx overestimated the true mean by 21%), with little dependence on the value of the ambient background O_3. This large overestimate of background O_3 by CAMx is very different than the results for El Paso background O_3.

Table 17. Ambient and CAMx GAM predictions for the 2019 background MDA8 O_3 (ppbv) for Houston based on the GAM model with the Is_Model variable.

	Ambient (Is_Model = 0)	CAMx (Is_Model = 1)	% Difference
Minimum	16.4	20.2	23%
25th Percentile	23.9	28.9	21%
Median	28.9	35.5	23%
Mean	31.0	37.6	21%
75th percentile	37.2	45.4	22%
Max	57.6	67.0	16%
Std. Dev.	9.1	11.0	

Table 18 shows the difference in smoke impacts calculated for 2019 days where the HMS indicated smoke over Houston. Note that this subset only includes 39 days. The GAMs trained on ambient data and the CAMx data make similar predictions for the fire impacts on these days, with the CAMx predictions generally being 2 ppbv larger but showing no dependence with the strength of the ambient fire impact. This suggests that the CAMx predictions of MDA8 O_3 on fire days overestimate the actual impacts of fires on background MDA8 O_3 in Houston.

Table 18. Estimated impact of smoke on the 2019 background MDA8 O_3 (ppbv) for Houston when calculated from Ambient and CAMx data.

	Ambient	CAMx
Minimum	5.6	8.4
25th Percentile	8.1	10.1
Median	9.2	11.1
Mean	9.7	11.6
75th percentile	10.9	13.0
Max	16.1	18.1
Std. Dev.	2.4	2.3

5 Quality Assurance

The processing and analysis scripts used in this project were inspected by a team member not involved in their creation for accuracy. All automated calculations and at least 10% of manual calculations will be inspected for correctness. This meets the requirement of Level III QAPPs that 10% of the data must be inspected.

Expert judgement was used to evaluate the reasonableness of the GAM fits for O_3 and STILT footprints. No concerning results were noted in these reviews.

The GAM fits for $PM_{2.5}$ show significant quality issues. The residuals are not normally distributed and show evidence of heteroskedacity. Various variable transforms did not remove these issues. Thus, the results of the $PM_{2.5}$ GAM analysis should be treated with caution, and only used to generate hypotheses about the smoke and dust impacts on $PM_{2.5}$ in Texas that need to be confirmed via other methods.

As the quality of the information, including secondary data, was not evaluated by EPA, the below disclaimer applies to all project deliverables:

Disclaimer: The information contained in this report or deliverable has not been evaluated by EPA for this specific application.

6 Conclusions

We performed a statistical analysis using generalized additive models (GAMs) to see how fires impacted background and maximum concentrations of O_3 and $PM_{2.5}$ in Houston and El Paso. Our results suggest that on days when the HMS indicated smoke over Houston and El Paso, the daily average $PM_{2.5}$ was elevated by 1.4-2.6 μg/m^3 on average (background and maximum) while the background MDA8 O_3 was elevated by 2.4-8 ppbv on average. Unfortunately, the results depend strongly on which set of fire predictors is used. For Houston, the change in O_3 impact as the smoke enters the city varies from -0.9 ppbv to +6.0 ppbv, with three out of four methods predicting an increase in mean O_3 as the smoke enters the city. In El Paso, the change in mean O_3 impact as the smoke enters the city varies from -1.6 ppbv to -0.5 ppbv. The geographic fire variables from Sec. 4.1.3 give the best fitting statistics and predicts fire impacts of 7.0-8.0 ppbv in both urban areas, with a slight decrease in the impact when the smoke enters the city.

We also performed a statistical analysis using generalized additive models (GAMs) to see if the CAMx predictions were consistent with the impact of fires on background and maximum concentrations of O_3 in Houston and El Paso. For El Paso, our analysis suggested that there were statistically significant differences between CAMx and the ambient data, but further analysis showed that the predicted impacts of fires in both cases were very similar. For Houston, however, the differences between CAMx and the ambient data fits were not statistically significant for maximum O_3, but the CAMx data strongly overestimates the background O_3 for Houston on both smoky and non-smoky days.

Since CAMx generally appears to give similar predictions for the impacts of smoke as the ambient data, there is little need to identify areas for improvement as called for in Objective 3 of this project. The exception is for the impacts of smoke on Houston background O_3, where CAMx predicts a 2 ppb larger impact. This is likely related to the general large overestimate of background O_3 by CAMx in Houston but may also be due to errors in the chemistry as emissions from the Yucatan interact with halogens over the Gulf.

In addition, our results showed that CAMx overestimates Houston background O_3 on both smoky and non-smoky days, suggesting that further work needs to be done on ozone-destroying halogen emissions and chemistry and on the biogenic emissions upwind of Houston. Similarly, the underpredictions of maximum O_3 in El Paso suggest that further work is needed on CAMx emissions for El Paso and Ciudad Juarez and the O_3 chemistry within the combined urban area.

7 Recommendations for Further Study

Future work should focus on finding ways to better determine the best set of smoke predictors for use in statistical studies such as this, with a focus on high tail events where smoke could lead to an exceedance of air quality standards using methods from Brown-Steiner et al. (2021). While the predictions of smoke impact on O_3 from CAMx appear to be reasonable based on this study, our results suggest that further work is needed to (a) address the overestimate of Houston background O_3 on both smoky and non-smoky days and (b) the underpredictions of maximum O_3 in El Paso.

8 References

Alvarado, M. J., C. R. Lonsdale, M. E. Mountain, & J. D. Hegarty (2015). *Investigating the Impact of Meteorology on O_3 and $PM_{2.5}$ Trends, Background Levels, and NAAQS Exceedances*, Final Report to Texas Commission on Environmental Quality (TCEQ) for Work Order No. 582-15-54118-01 under TCEQ Contract No. 582-15-50415, August 31.

Alvarado, M. J., K. Barsanti, S. Chung, D. Jaffe, & T. Moore (2022). "Smoke Chemistry", in *Wildland fire smoke in the United States: a scientific assessment*, Peterson, D.L.; McCaffrey, S.M.; Patel-Weynand, T., eds. Dordrecht: The Netherlands, ISBN-13: 978-3030870447.

Baker, K. R., Woody, M. C., Tonnesen, G. S., Hutzell, W., Pye, H. O. T., Beaver, M. R., Pouliot, G., & Pierce, T. (2016). Contribution of regional-scale fire events to ozone and $PM_{2.5}$ air quality estimated by photochemical modeling approaches. *Atmos. Environ., 140*, 539–554. doi:10.1016/j.atmosenv.2016.06.032

Brey, S. J., Ruminski, M., Atwood, S. A., and Fischer, E. V. (2018), Connecting smoke plumes to sources using Hazard Mapping System (HMS) smoke and fire location data over North America, *Atmos. Chem. Phys.*, 18, 1745–1761, https://doi.org/10.5194/acp-18-1745-2018.

Brown-Steiner, B., Zhou, X., Alvarado, M. J., & Russell, B. T. (2021). Prediction of High-ozone Events Using GAM, SMOTE, and Tail Dependence Approaches in Texas (2005-2019). *Aerosol and Air Quality Research*, *21*, 210077.

Camalier, L., Cox, W., & Dolwick, P. (2007). The effects of meteorology on ozone in urban areas and their use in assessing ozone trends. *Atmos. Environ.*, *41*(33), 7127-7137.

Dayalu, A., Alvarado, M. J., & Sun, Q. (2021). *Using Satellite Observations to Quantify Surface $PM_{2.5}$ Impacts from Biomass Burning Smoke*, Final Report to Texas Air Quality Research Program (AQRP) Project 20-005, August 31.

de Foy, B., Saroar, M. G., Salam, A., & Schauer, J. J. (2021). Distinguishing Air Pollution Due to Stagnation, Local Emissions, and Long-Range Transport Using a Generalized Additive Model to Analyze Hourly Monitoring Data. *ACS Earth and Space Chemistry*, *5*(9), 2329-2340.

Draxler, R. R., & Hess, G. D. (1998). An overview of the HYSPLIT_4 modelling system for trajectories. *Australian meteorological magazine*, *47*(4), 295-308.

Gong, X., Kaulfus, A., Nair, U., & Jaffe, D. A. (2017). Quantifying O_3 impacts in urban areas due to wildfires using a generalized additive model. *Environ. Sci. & Technol.*, *51*(22), 13216-13223.

Hu, X., Yu, C., Tian, D., Ruminski, M., Robertson, K., Waller, L. A., and Liu, Y. (2016), Comparison of the Hazard Mapping System (HMS) fire product to ground-based fire records in Georgia, USA, *J. Geophys. Res.-Atmos.*, 121, 2015JD024448, https://doi.org/10.1002/2015JD024448.

Lin, J. C., Gerbig, C., Wofsy, S. C., Andrews, A. E., Daube, B. C., Davis, K. J., & Grainger, C. A. (2003). A near-field tool for simulating the upstream influence of atmospheric observations: The Stochastic Time-Inverted Lagrangian Transport (STILT) model. *Journal of Geophysical Research: Atmospheres*, *108*(D16).

McDonald-Buller, E., Y. Kimura, C. Wiedinmyer, C. Emery, Z. Liu, and G. Yarwood (2015), *Targeted Improvements in the Fire Inventory form NCAR (FINN) Model for*

Texas Air Quality Planning, Final Report to Texas Air Quality Research Program (AQRP) for Project 14-011, December 2015.
McVey, A., R. Pernak, J. Hegarty, & M. Alvarado (2018). *El Paso Ozone and $PM_{2.5}$ Background and Totals Trend Analysis*, Final Report to Texas Commission on Environmental Quality (TCEQ) for Work Order No. 582-18-81763-07 under TCEQ Contract No. 582-15-50414, June 29.
Nehrkorn, T., Eluszkiewicz, J., Wofsy, S. C., Lin, J. C., Gerbig, C., Longo, M., & Freitas, S. (2010). Coupled weather research and forecasting–stochastic time-inverted lagrangian transport (WRF–STILT) model. *Meteorology and Atmospheric Physics*, *107*(1), 51-64.
Pernak, R., Alvarado, M., Lonsdale, C., Mountain, M., Hegarty, J., & Nehrkorn, T. (2019). Forecasting surface O_3 in Texas urban areas using random forest and generalized additive models. *Aerosol and Air Quality Research*, *19*(12), 2815-2826.
Rolph, G. D., Draxler, R. R., Stein, A. F., Taylor, A., Ruminski, M. G., Kondragunta, S., Zeng, J., Huang, H.-C., Manikin, G., McQueen, J. T., and Davidson, P. M. (2009), Description and verification of the NOAA smoke forecasting system: The 2007 fire season, *Weather Forecast.*, 24, 361–378, https://doi.org/10.1175/2008WAF2222165.1.
Ruminski, M., Kondragunta, S., Draxler, R., and Zeng, J. (2006), Recent changes to the Hazard Mapping System, 15th Int. Emiss. Inventory Conf, (Reinventing Inventories), available at: https://www.researchgate.net/publication/228625934_Recent_changes_to_the_Hazard_Mapping_System (last access: 11 January 2020).
Schroeder, W., Ruminski, M., Csiszar, I., Giglio, L., Giglio, E., Schmidt, C., and Morisette, J. (2008), Validation analyses of an operational fire monitoring product: The Hazard Mapping System, *Int. J. Remote Sens.*, 29, 6059–6066.
Wiedinmyer, C., Akagi, S. K., Yokelson, R. J., Emmons, L. K., Al-Saadi, J. A., Orlando, J. J., & Soja, A. J. (2011). The Fire INventory from NCAR (FINN): A high resolution global model to estimate the emissions from open burning. *Geoscientific Model Development*, *4*(3), 625-641.
Wood, S. N. (2006). *Generalized additive models: An introduction with R*. Chapman and Hall/CRC.